
Resistive Hot Accretion Flows with Anisotropic Pressure

S. M. Ghoreyshi • A. R. Khesali

smghoreyshi64@gmail.com

Abstract

Since the collisional mean free path of charged particles in hot accretion flows can be significantly larger than the typical length-scale of the accretion flows, the gas pressure is anisotropic to magnetic field lines. For such a large collisional mean free path, the resistive dissipation can also play a key role in hot accretion flows. In this paper, we study the dynamics of resistive hot accretion flows in the presence of anisotropic pressure. We present a set of self-similar solutions where the flow variables are assumed to be a function only of radius. Our results show that the radial and rotational velocities and the sound speed increase considerably with the strength of anisotropic pressure. The increase in infall velocity and in sound speed are more significant if the resistive dissipation is taken into account. We find that such changes depend on the field strength. Our results indicate that the resistive heating is 10% of the heating by the work done by anisotropic pressure when the strength of anisotropic pressure is 0.1. This value becomes higher when the strength of anisotropic pressure reduces. The increase in disk temperature can lead to heating and acceleration of the electrons in such flows. It helps us to explain the origin of phenomena such as the flares in Galactic Center Sgr A*.

Keywords accretion, accretion disks; magnetic field, diffusion; stars: winds, outflows

1 Introduction

In standard accretion disks (Shakura and Sunyaev 1973), advection is not considered and the energy released due to dissipative process is radiated away. The standard disks are relatively cold and cannot explain some phenomena in systems such as Galactic Center Sgr A* (Kato et al. 2008). Therefore, other models such as the radiatively inefficient accretion flow (RIAF) model have been introduced (Narayan and Yi 1994; Kato et al. 2008). In such disks, the released energy is retained within the accreting flows and is advected radially inward. This leads to hot accretion flows and produces high-energy emission. In addition to extremely low-luminosity active galactic nuclei (LLAGNs) such as Sgr A* (Yuan et al. 2002; Yuan and Narayan 2014) and M 87 (Park et al. 2019), hot accretion flows can be an appropriate model to the quiescent and hard states of black hole X-ray binaries (Done et al. 2007; Qiao and Liu 2009; Zhang et al. 2012; Yan and Yu 2017).

The numerical simulations have revealed that strong outflows can be launched in hot accretion flows (Ohsuga et al. 2009; Yuan et al. 2012,?, 2015; Bu et al. 2016a,b). The presence of outflows has also been confirmed by the observations of LLAGNs and X-ray binaries (Tombesi et al. 2010; Crenshaw and Kraemer 2012; Wang et al. 2013; Tombesi et al. 2014; Cheung et al. 2016; Homan et al. 2016; Ma et al. 2019; Park et al. 2019). The outflows can extract mass, angular momentum and energy from the disk (Pudritz 1985; Knigge 1999; Xue and Wang 2005; Cao 2016; Cao and Lai 2019) and strongly affect the structure of accreting flows. For instance, the disk gas surrounding the black hole can be pushed away by the outflows. This extraction causes the accretion rate of the black hole to decrease (Yuan et al. 2018; Bu and Yang 2019). Several attempts to explore the effects of outflow

S. M. Ghoreyshi

A. R. Khesali

Department of Physics, University of Mazandaran, Babolsar, Iran.

on the dynamics of hot accretion flows have been made over the last several years. The results of previous works indicate that the outflows can be an effective cooling agent in hot accretion flows (e.g., Bu et al. 2009; Mosallanezhad et al. 2013; Bu et al. 2019; Ghoreyshi and Shadmehri 2020).

Recent findings indicate that there is an orbiting hot spot nearby the event horizon of Sgr A* (Gravity Collaboration et al. 2018). Non-thermal emission related to such hot spots is believed to be due to magnetic reconnection (Ding et al. 2010; Ripperda et al. 2019b) and the ideal MHD is unable to explain non-thermal emission. We require dissipative (non-ideal) mechanisms to describe such observational phenomena in accretion systems. There are three regimes in non-ideal MHD due to the relative drifts of different charged species with respect to the neutral particles; ohmic dissipation, Hall effect, and ambipolar diffusion. Although ohmic dissipation leading to a decoupling of the magnetic field from all charged particles can be important in the innermost parts of the disks around protostars, ambipolar diffusion is the dominant non-ideal MHD effect in the outer regions of such disks and causes the magnetic field to decouple from the neutral gas. But the Hall effect occurs when the magnetic field decouples from ions and charged dust grains. This non-ideal effect, which is an intermediate regime between ambipolar diffusion and ohmic resistivity, plays an important role at other parts of such disks (see Braiding and Wardle 2012).

Flows of disks around dwarf novae (Fleming et al. 2000; Sano and Stone 2002; Scepi et al. 2018) and protoplanetary disks (Béthune et al. 2017; Mori et al. 2019; Wang et al. 2019; Das and Basu 2021) which are cold and partially ionized can be affected by all of these non-ideal effects. However, gas present in RIAFs is hot and fully ionized and ambipolar diffusion in high ionization state is negligible. Furthermore, the mean free path for the Coulomb interactions in hot accretion flows is larger than the typical length-scale of the system, the Coulomb coupling between ions and electrons is not strong enough and such flows are effectively collisionless (Quataert 1998). Therefore, the gyration timescale in these flows is much shorter than the dynamical timescale and the Hall effect can be safely ignored (see Pandey and Wardle 2008). Hence, inclusion of resistivity is essential to trigger the magnetic reconnection (e.g., Ding et al. 2010; Ripperda et al. 2019a, 2020).

Much effort has been devoted to the study of resistivity in hot accretion flows, and interesting results have been obtained. For example, Zahra Zeraatgari et al. (2018) showed that the ohmic resistivity in such flows

modifies the amount of magnetic field and the role of the magnetic field in transferring angular momentum. Abbassi and Mosallanezhad (2012) also showed that the rotational velocity of the resistive accretion flows in the absence of outflow depends on the magnetic diffusivity. They found that the effect of magnetic diffusivity on the rotational velocity depends on the field components (see also Ghoreyshi 2020). In the presence of outflows, the results indicate that the rotational velocity of hot accretion flows is always sub-Keplerian and the disk reaches a non-rotating limit when the magnetic diffusivity increases (Ghoreyshi 2020). We know that the magnetic diffusivity not only modifies the structure of accretion flows, but also can affect wind launching and the strength of the disk wind (Kuwabara et al. 2000; Fendt and Čemeljić 2002; Igumenshchev et al. 2003; Čemeljić et al. 2014; Qian et al. 2018; Vourellis et al. 2019). On the other hand, the magnetic dissipation heating in regions of a disk where outflows may play an important role is comparable to the viscous heating (Zahra Zeraatgari et al. 2018). This heating mechanism helps the electron to have a higher temperature (Bisnovatyi-Kogan and Lovelace 1997; Ding et al. 2010). Hence, the magnetic diffusivity can be an important mechanism in hot accretion flows.

As mentioned above, the Coulomb collision mean free path of charged particles (both electrons and ions) in the accretion flow of extremely LLAGNs, such as Sgr A* and M 87, is much larger than the typical size of the system (see Bu et al. 2019). In such weakly-collisional flows, anisotropic thermal conduction can be significant and along the magnetic field lines (Parrish and Stone 2007; Sharma et al. 2008; Bu et al. 2011). The anisotropic thermal conduction plays an important role in the transport of thermal energy from the inner (hotter) to the outer (cooler) parts. Thus, the anisotropic thermal conduction affects the properties of outflow such as the energy flux (Bu et al. 2016). Since the ions' mean free path in weakly-collisional accretion flows is larger than its Larmor radius, the pressure perpendicular to the magnetic field line and that parallel to the magnetic field line are not the same (Quataert et al. 2002; Sharma et al. 2003; Chandra et al. 2015). Previous findings indicate that the properties of a hot accretion flow depend significantly on anisotropic pressure. For example, the mass inflow rate in hot accretion flows with the anisotropic pressure decreases towards the central object when a very weak magnetic field is present (Wu et al. 2017). By considering a relatively strong magnetic field, Bu et al. (2019) found that the infall velocity increases with the anisotropic pressure and with the outflows. We know that the changes in the infall velocity due to the outflow are dependent on

the magnetic diffusivity when the anisotropic pressure is absent (Ghoreyshi 2020). To the best of our knowledge, the effect of magnetic diffusivity on the properties of hot accretion flows with the anisotropic pressure has not yet been studied in detail. Here, we will study the dynamics of resistive hot accretion flows in the presence of anisotropic pressure. Indeed, our main aim is to explore the role of magnetic diffusivity and compare the resistive heating with the other heating mechanisms.

Here, the magnetic field is assumed to have only a ϕ -component. We present the self-similar solutions of resistive hot accretion flows when the outflows are present. The paper is organized as follows. We first formulate basic equations for such a disk in Sect. 2. In Sect. 3, the basic equations are solved using self-similar method and the results are discussed in Sect. 4. We then summarize our conclusions in the final section.

2 Basic Equations

In this paper, we study the time-steady ($\partial/\partial t = 0$) and the axisymmetric ($\partial/\partial\phi = 0$) resistive hot accretion flows in the cylindrical coordinates (r, ϕ, z) . All flow variables are assumed to depend only on r . The basic equations in Gaussian units are as follows:

$$\frac{d\rho}{dt} + \rho \nabla \cdot \mathbf{v} = 0, \quad (1)$$

$$\rho \frac{d\mathbf{V}}{dt} = -\nabla p - \rho \nabla \Phi + \frac{1}{4\pi} (\nabla \times \mathbf{B}) \times \mathbf{B} + \nabla \cdot \mathbf{T} + \nabla \cdot \mathbf{\Pi}, \quad (2)$$

$$\rho \left(\frac{de}{dt} - \frac{p}{\rho^2} \frac{d\rho}{dt} \right) = (q_{\text{vis}} + q_B) - q_{\text{rad}}, \quad (3)$$

$$\frac{\partial \mathbf{B}}{\partial t} = \nabla \times (\mathbf{v} \times \mathbf{B} - \eta \nabla \times \mathbf{B}), \quad (4)$$

where $d/dt = \partial/\partial t + \mathbf{v} \cdot \nabla$ is the Lagrangian time derivative. Here, ρ and $\mathbf{v} = (v_r, v_\phi, 0)$ are the midplane density of the disk and the velocity vector, respectively. p is the gas pressure and Φ is the gravitational potential. We ignore relativistic effects and use Newtonian gravity ($\Phi = -GM_*/r$). From the numerical MHD simulations done by Hirose et al. (2004), the magnetic field in the main disk body, corona, and inner torus is mainly toroidal. But the poloidal component can be important in regions near the black hole. Hence, we assume that the dominant field component in most regions of the accretion flow is toroidal. In the present

paper, therefore, a large-scale magnetic field is adopted that has only a toroidal component B_ϕ . In Eq. (4), η is the magnetic diffusivity.

The fourth term on the right side of Eq. (2), $\nabla \cdot \mathbf{T}$, represents the angular momentum transferred by the turbulent magnetic field. If the $r\phi$ -component of the viscous stress tensor in an accretion disk is dominant, we have (Kato et al. 2008)

$$T_{r\phi} = \rho \nu_1 r \left(\frac{d\Omega}{dr} \right), \quad (5)$$

where $\nu_1 = \alpha_1 c_s H$. Here, H is disk half-thickness, and $c_s = \sqrt{p/\rho}$ is sound speed. When the magnetic fields exist in an accretion disk, both c_s and H are written as a function of the magnetic field strength. Therefore, we cannot adopt the simple form $\nu_1 = \alpha c_s^2 / \Omega_K$ for the viscosity. In our paper, we will compare the results of these two forms of viscosity (see Fig. 1).

The anisotropic pressure $\mathbf{\Pi}$ in Eq. (2) which can be denoted by an anisotropic viscosity is written as (Braginskii 1965; Balbus 2004; Chandra et al. 2015)

$$\mathbf{\Pi} = -3\rho\nu_2 \left[\mathbf{bb} : \nabla \mathbf{v} - \frac{\nabla \cdot \mathbf{v}}{3} \mathbf{I} \right] \left[\mathbf{bb} - \frac{\mathbf{I}}{3} \right]. \quad (6)$$

Here, $\mathbf{b} = \mathbf{B}/|\mathbf{B}|$ and \mathbf{I} are the unit vector in magnetic field direction and the unit tensor, respectively. The anisotropic viscosity ν_2 is also written as $\alpha_2 c_s H$ in which α_2 represents the strength of anisotropic pressure. When the magnetic field has only a toroidal component, the non-zero components of the anisotropic pressure are as follows (Bu et al. 2019),

$$\Pi_{rr} = \Pi_{zz} = -\frac{1}{2} \Pi_{\phi\phi} = -\frac{\rho \nu_2 r^2}{3} \frac{d}{dr} \left(\frac{v_r}{r^2} \right), \quad (7)$$

where v_r is the radial infall velocity. Since the magnetic field geometry modifies the anisotropic pressure tensor, the components of anisotropic pressure can be very complicated in the presence of a poloidal magnetic field. Therefore, we consider the dominant component of the magnetic field, i.e., the toroidal component, for simplicity.

In Eq. (3), e , q_{vis} , q_B , and q_{rad} represent the gas specific internal energy, the heating rate of the gas, the resistive heating, and the radiative cooling rates, respectively. We assume that the right side of Eq. (3) is equal to $f(q_{\text{vis}} + q_B)$ in which the advection factor can be in the range $0 \leq f \leq 1$. In this paper, we set $q_{\text{rad}} = 0$, and then the advection factor $f = 1.0$. The gas heating rate q_{vis} is the sum of the heating by the magnetic reconnection due to the turbulent component of the magnetic field ($q_{\text{vis}1}$) and the heating by the work done by anisotropic pressure ($q_{\text{vis}2}$). These heating rates are defined by

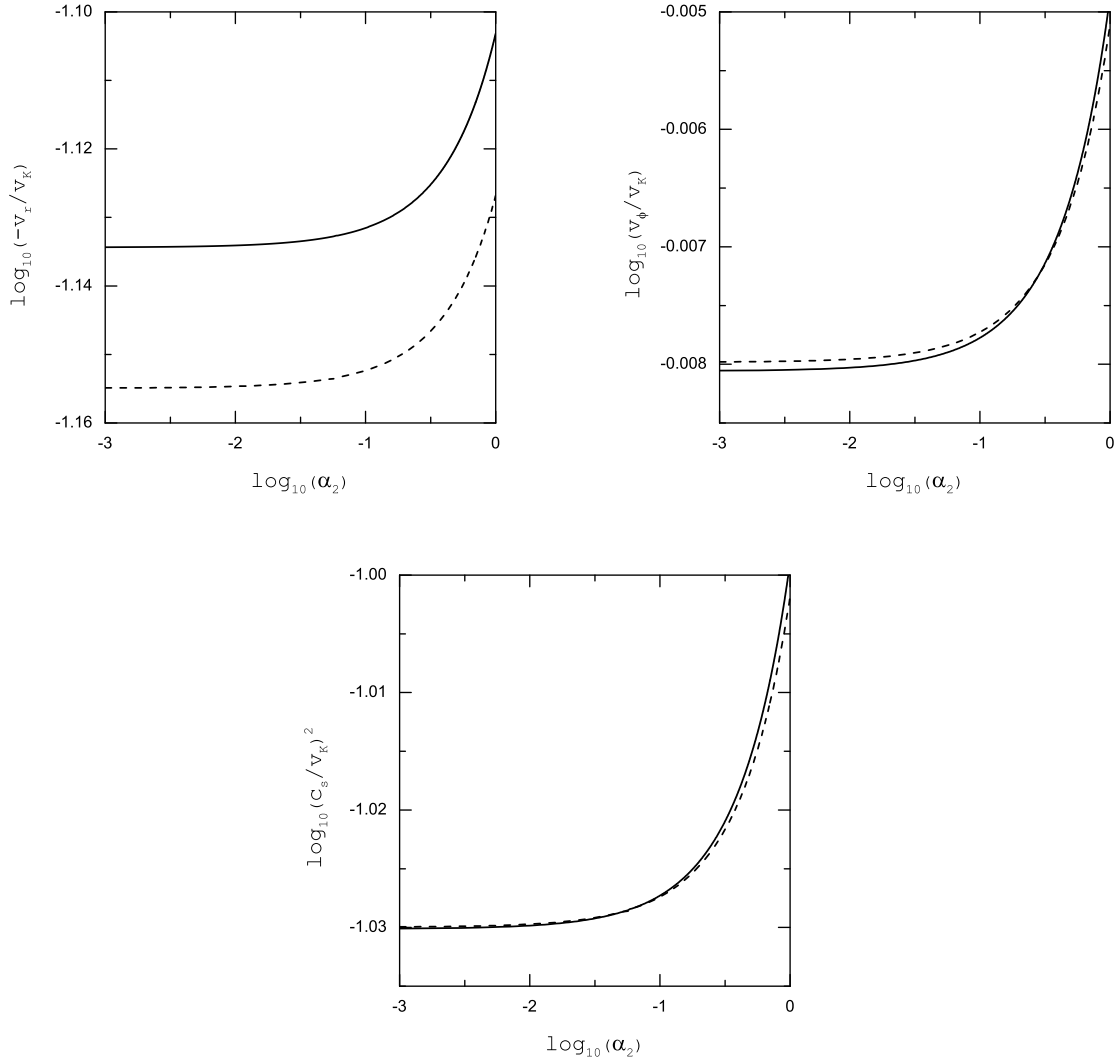


Fig. 1 Profiles of the physical variables of the accretion disk versus the strength of anisotropic pressure. A comparison between two forms of the viscosity ν for $\gamma = 4/3$, $s = 1/2$, $\alpha_1 = 0.1$, $\beta_\phi = 0.1$, $\zeta_1 = \zeta_2 = \zeta_3 = 1.2$. While the solid curves correspond to the definition of $\nu = \alpha c_s H$, the dashed curves show the results of $\nu = \alpha c_s^2 / \Omega_K$

$$q_{\text{vis1}} = \rho\nu_1 r^2 \left(\frac{d\Omega}{dr} \right)^2$$

and

$$q_{\text{vis2}} = \frac{1}{3} \rho\nu_2 r^4 \left[\frac{d}{dr} \left(\frac{v_r}{r^2} \right) \right]^2,$$

where $\Omega = v_\phi/r$ is the angular velocity of the gas and v_ϕ is the rotational velocity. The resistive heating rate is also written as

$$q_B = \frac{\eta}{4\pi} |\nabla \times \mathbf{B}|^2.$$

The diffusivity is believed to be generated by turbulence triggered within the accretion disk (Zanni et al. 2007). Hence, we assume that the anomalous magnetic diffusivity η can be expressed in the same way as in Bisnovatyi-Kogan and Ruzmaikin (1976), namely,

$$\eta = \eta_0 c_s H,$$

where the α -prescription of Shakura and Sunyaev (1973) is adopted and the magnetic diffusivity parameter η_0 is a constant, less than unity. Note that this form of the magnetic diffusivity was used in some previous work (e.g., Shadmehri 2004; Abbassi and Mosallanezhad 2012; Samadi et al. 2014), although H was replaced by c_s/Ω_K in the definition of η .

According to the above relations, the radial and azimuthal momentum equations and the energy equation in the presence of outflow are written as

$$\begin{aligned} v_r \frac{dv_r}{dr} + \frac{1}{2\pi r \Sigma} \frac{d\dot{M}}{dr} (v_{rw} - v_r) &= \frac{v_\phi^2}{r} - \frac{GM_*}{r^2} \\ - \frac{1}{\Sigma} \frac{d}{dr} (\Sigma c_s^2) - \frac{1}{2\Sigma} \frac{d}{dr} (\Sigma c_\phi^2) - \frac{c_\phi^2}{r} \\ + \frac{2v_r}{3r^2 \Sigma} \left[\nu_2 \Sigma + \frac{d}{dr} (r\nu_2 \Sigma) \right] \\ - \frac{1}{3r \Sigma} \frac{d}{dr} (r\nu_2 \Sigma \frac{dv_r}{dr}), \end{aligned} \quad (8)$$

$$\begin{aligned} \frac{\Sigma v_r}{r} \frac{d}{dr} (rv_\phi) + \frac{1}{2\pi r \Sigma} \frac{d\dot{M}}{dr} (v_{\phi w} \\ - v_\phi) &= \frac{1}{r^2} \frac{d}{dr} (r^3 \nu_1 \Sigma \frac{d\Omega}{dr}), \end{aligned} \quad (9)$$

$$\begin{aligned} \frac{v_r}{\gamma - 1} \frac{dc_s^2}{dr} - \frac{v_r c_s^2}{\rho} \frac{d\rho}{dr} + \frac{1}{2\pi r \Sigma} \frac{d\dot{M}}{dr} (e_w - e) \\ = f \left\{ r^2 \nu_1 \left(\frac{d\Omega}{dr} \right)^2 + \frac{1}{3} r^4 \nu_2 \left[\frac{d}{dr} \left(\frac{v_r}{r^2} \right) \right]^2 \right. \\ \left. + \frac{\eta}{4\pi \rho} \left[\frac{1}{r} \frac{d}{dr} (rB_\phi) \right]^2 \right\}, \end{aligned} \quad (10)$$

where the surface density Σ and the Alfvén sound speed c_ϕ are defined as $\Sigma = 2\rho H$, and $c_\phi^2 = B_\phi^2/4\pi\rho$. v_{rw} and $v_{\phi w}$ denote the r - and ϕ -components of the velocity of the outflow. e_w is the specific internal energy of the outflow. In the present paper, we assume $v_{rw} = \zeta_1 v_r$, $v_{\phi w} = \zeta_2 v_\phi$, and $e_w = \zeta_3 e$ (Bu et al. 2009).

The hydrostatic balance in the vertical direction leads to a relation between H and $c_{s,\phi}$. We have

$$\frac{GM_*}{r^3} H^2 = c_s^2 (1 + \beta_\phi), \quad (11)$$

where β_ϕ is the ratio of the magnetic pressure to the gas pressure, i.e., $\beta_\phi = (1/2)(c_\phi/c_s)^2$, which can describe the strength of the large-scale magnetic field. For hot accretion flows, β_ϕ may lie in the range from 0.01 to 1 (e.g. De Villiers et al. 2003; Beckwith et al. 2008).

3 Self-similar solutions

As mentioned earlier, the variables of the disk are assumed to be as a function of r . We use self-similar solutions in the following forms (Narayan and Yi 1994):

$$v_r(r) = -C_1 \alpha_1 v_K, \quad (12)$$

$$v_\phi(r) = C_2 v_K, \quad (13)$$

$$c_s^2(r) = C_3 v_K^2. \quad (14)$$

By using the form $\Sigma = \Sigma_0 r^s$ for the surface density and the definition of \dot{M} ($= -2\pi r \Sigma v_r$), the accretion rate takes the form

$$\dot{M} = 2\pi \alpha_1 C_1 \Sigma_0 \sqrt{GM_*} r^{s+\frac{1}{2}}.$$

Here, Σ_0 and s are two physical constants and s is between $-1/2$ and $1/2$. We note that $s = -1/2$ corresponds to the cases without outflow. By substituting these self-similar solutions into the basic Eqs. (8)–(10) and using Eq. (11), we have

$$\begin{aligned} - \left[\frac{1}{2} + (s + \frac{1}{2})(\zeta_1 - 1) \right] \alpha_1^2 C_1^2 &= C_2^2 - 1 \\ - 2\beta_\phi C_3 - (s - 1)(1 + \beta_\phi) C_3 \\ - \frac{5}{6} \alpha_1 \alpha_2 \sqrt{1 + \beta_\phi} (s + 2) C_1 C_3, \end{aligned} \quad (15)$$

$$\left[1 - (2s + 1)(\zeta_2 - 1) \right] C_1 = 3\sqrt{1 + \beta_\phi} (s + 1) C_3, \quad (16)$$

$$\begin{aligned} \left[\frac{1}{\gamma - 1} + s - 1 + \frac{(2s + 1)(\zeta_3 - 1)}{2(\gamma - 1)} \right] C_1 = f \\ \times \sqrt{1 + \beta_\phi} \left(\frac{9}{4} C_2^2 + \frac{25}{12} \alpha_1 \alpha_2 C_1^2 + \frac{\beta_\phi \eta_0 s^2}{2\alpha_1} C_3 \right). \end{aligned} \quad (17)$$

Adopting an odd function of z for B_ϕ and a simple form of the viscosity, Eqs. (15)–(17) in the absence of magnetic diffusivity reduce to Eqs. (19), (20), and (22)

of [Bu et al. \(2019\)](#). If the parameters s , α_1 , α_2 , β_ϕ , η_0 , ζ_1 , ζ_2 , ζ_3 , and γ have given values, there is a closed set of equations for C_1 , C_2 , and C_3 to determine the variables of the accretion flow. By using the above equations, a second-order algebraic equation for C_1 is obtained as follows:

$$\left\{ \frac{5(s+2) \left[1 + (2s+1)(1-\zeta_2) \right] \alpha_1 \alpha_2}{8(s+1)} - \frac{9 \left[1 + (2s+1)(\zeta_1-1) \right] \alpha_1^2}{8} + \frac{25\alpha_1 \alpha_2}{12} \right\} C_1^2 + \left\{ -\frac{1}{f\sqrt{1+\beta_\phi}} \left[s-1 + \frac{(2s+1)(\zeta_3-1)}{2(\gamma-1)} + \frac{1}{\gamma-1} \right] + \left[\frac{1+(2s+1)(1-\zeta_2)}{2(s+1)} \right] \times \left[\frac{3\beta_\phi}{\sqrt{1+\beta_\phi}} + \frac{3(s-1)\sqrt{1+\beta_\phi}}{2} \right] - \frac{\beta_\phi \eta_0 s^2}{3\sqrt{1+\beta_\phi} \alpha_1} \right\} C_1 + \frac{9}{4} = 0. \quad (18)$$

Noting that the resistive heating rate is proportional to $\beta_\phi \eta_0 s^2$ (see the last term on the right side of Eq. (17)); we will discuss the role of each of these parameters. Here, we focus on the effects η_0 , β_ϕ , s , and α_2 . The other parameters are assumed to be constant; $\gamma = 4/3$, $f = 1$, $\alpha_1 = 0.1$, and $\zeta_1 = \zeta_2 = \zeta_3 = 1.2$. By setting these parameters, Eqs. (15)–(17) lead to the dependence of C_2 and C_3 on C_1 as follows:

$$C_2 = \left[1 - \frac{\sqrt{1+\beta_\phi}(0.8-0.4s)(1-s)C_1}{3(s+1)} + \frac{2\beta_\phi(0.8-0.4s)C_1}{3\sqrt{1+\beta_\phi}(s+1)} - 0.005(1.2+0.4s)C_1^2 + \frac{0.028\alpha_2(0.8-0.4s)(s+2)C_1^2}{s+1} \right]^{1/2}, \quad (19)$$

$$C_3 = \frac{(0.8-0.4s)}{3\sqrt{1+\beta_\phi}(s+1)} C_1. \quad (20)$$

Here, C_1 is obtained by solving Eq. (18).

4 Results

In order to examine the effects of anisotropic pressure on the properties of a resistive hot accretion flow, we obtain the variables C_1 , C_2 , and C_3 as a function of the strength of anisotropic pressure α_2 . In this paper, the strength of anisotropic pressure is assumed to be in the

range from 0.001 to 1.0. The other input parameters are $\eta_0 = 0.1$, $s = 0.5$, and $\beta_\phi = 0.1$, unless stated otherwise. Since [Bu et al. \(2019\)](#) studied the effect of parameters ζ_1 , ζ_2 , and ζ_3 on the disk properties, these parameters, as mentioned above, are assumed to be fixed. We also note that only real roots corresponding to positive C_2^2 must be adopted.

As mentioned previously, the viscosity in the magnetized disk does not obey the form $\nu = \alpha c_s^2 / \Omega_K$. According to $\nu = \alpha c_s H$ and Eq. (11), the viscosity in the magnetized disk is defined as $\nu = \alpha \sqrt{1 + \beta_\phi} c_s^2 / \Omega_K$. For now, we will compare the viscosities $\nu = \alpha c_s H$ and $\nu = \alpha c_s^2 / \Omega_K$. In Fig. 1, the results of this comparison are illustrated. Here, we assume that $s = 1/2$, $\alpha_1 = 0.1$, $\beta_\phi = 0.1$, $\zeta_1 = \zeta_2 = \zeta_3 = 1.2$. All profiles are displayed as a function of the strength of anisotropic pressure α_2 . We find that the disk variables effectively are enhanced as the strength of anisotropic pressure increases. The strength of the anisotropic pressure is one of the important parameters in the heating by anisotropic pressure. Since the sound speed is proportional to $T^{1/2}$, one can expect that the sound speed increases with the strength of the anisotropic pressure. The last term on the right-hand side of Eq. (15) is the force of the divergence of the anisotropic pressure. For our input parameters, this force is always negative. This means that the direction of the force of the divergence of the anisotropic pressure is towards the central object. According to Eq. (15), an increase in the strength of the anisotropic pressure causes this force, and thus the radial infall velocity, to increase (see also [Bu et al. 2019](#)). By solving Eqs. (15)–(17), we find that the rotational velocity is an increasing function of α_2 (see Eq. (19)). This increasing trend is seen in the top right panel of Fig. 1.

The top left panel in Fig. 1 is the normalized radial infall velocity (v_r/v_K). We find that the modified viscosity $\nu = \alpha \sqrt{1 + \beta_\phi} c_s^2 / \Omega_K$ increases the infall velocity. One can expect that the value of β_ϕ plays a key role in these changes (see also [Zhang and Dai 2008](#)). Although this increase occurs within all α_2 , the strength of the anisotropic pressure affects these changes. When α_2 rises, the increase in infall velocity is more significant. The modification of the viscosity does not significantly change the rotational velocity (top right panel) and the sound speed (bottom panel). In the high- α_2 limit, these velocities increase due to the modified viscosity. By reducing α_2 , the modified viscosity causes the rotational velocity and the sound speed to reduce. Our results in the low- α_2 limit are in good agreement with the findings of [Zhang and Dai \(2008\)](#). They also pointed out that the modified viscosity decreases the radial velocity and the sound speed. We will apply the modified viscosity form $\nu = \alpha \sqrt{1 + \beta_\phi} c_s^2 / \Omega_K$ to the profiles in the next figures.

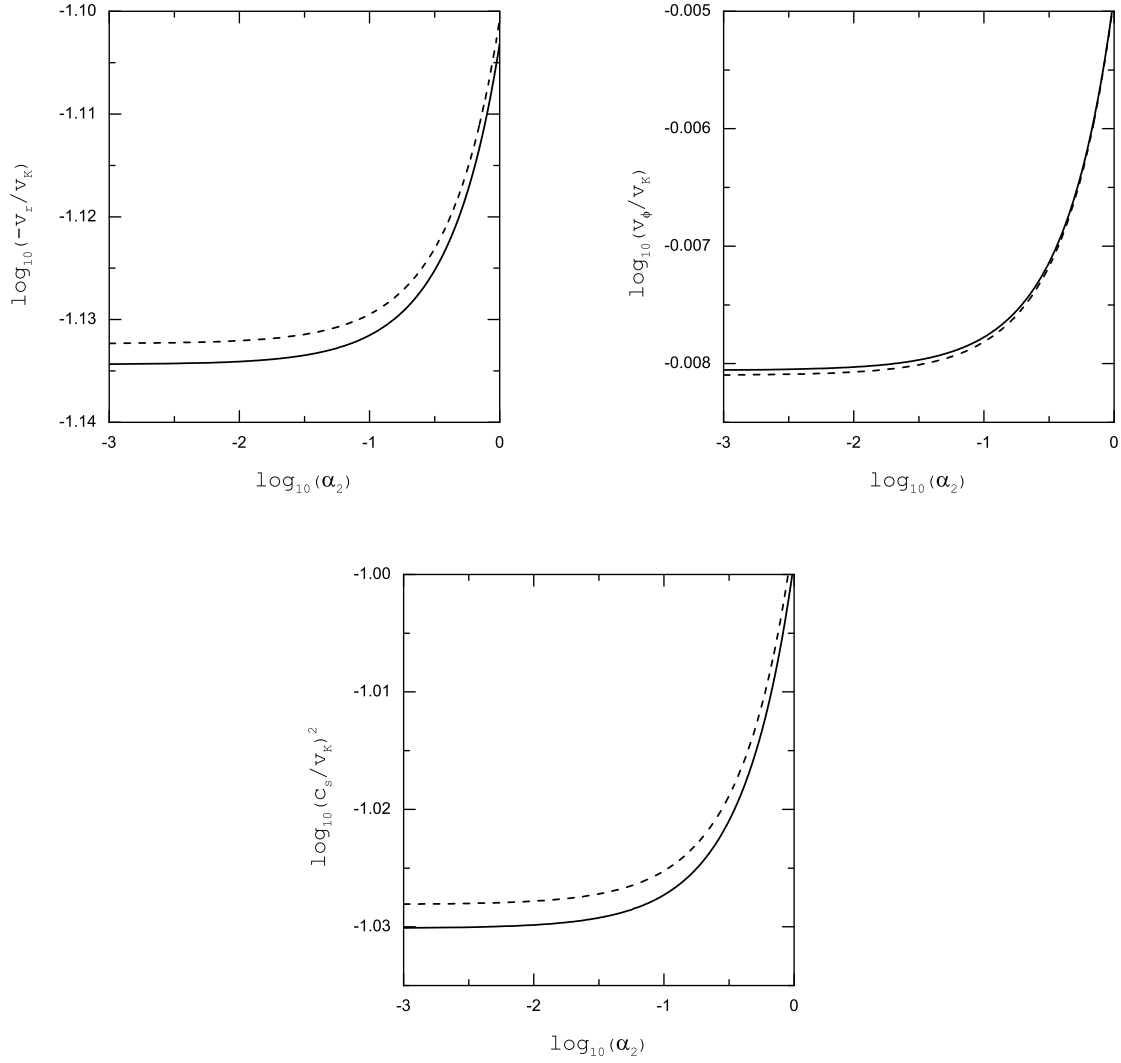


Fig. 2 Profiles of the physical variables of the accretion disk versus the strength of anisotropic pressure for different values of η_0 . The solid and the dashed curves correspond to $\eta_0 = 0.1$ and 1.0, respectively

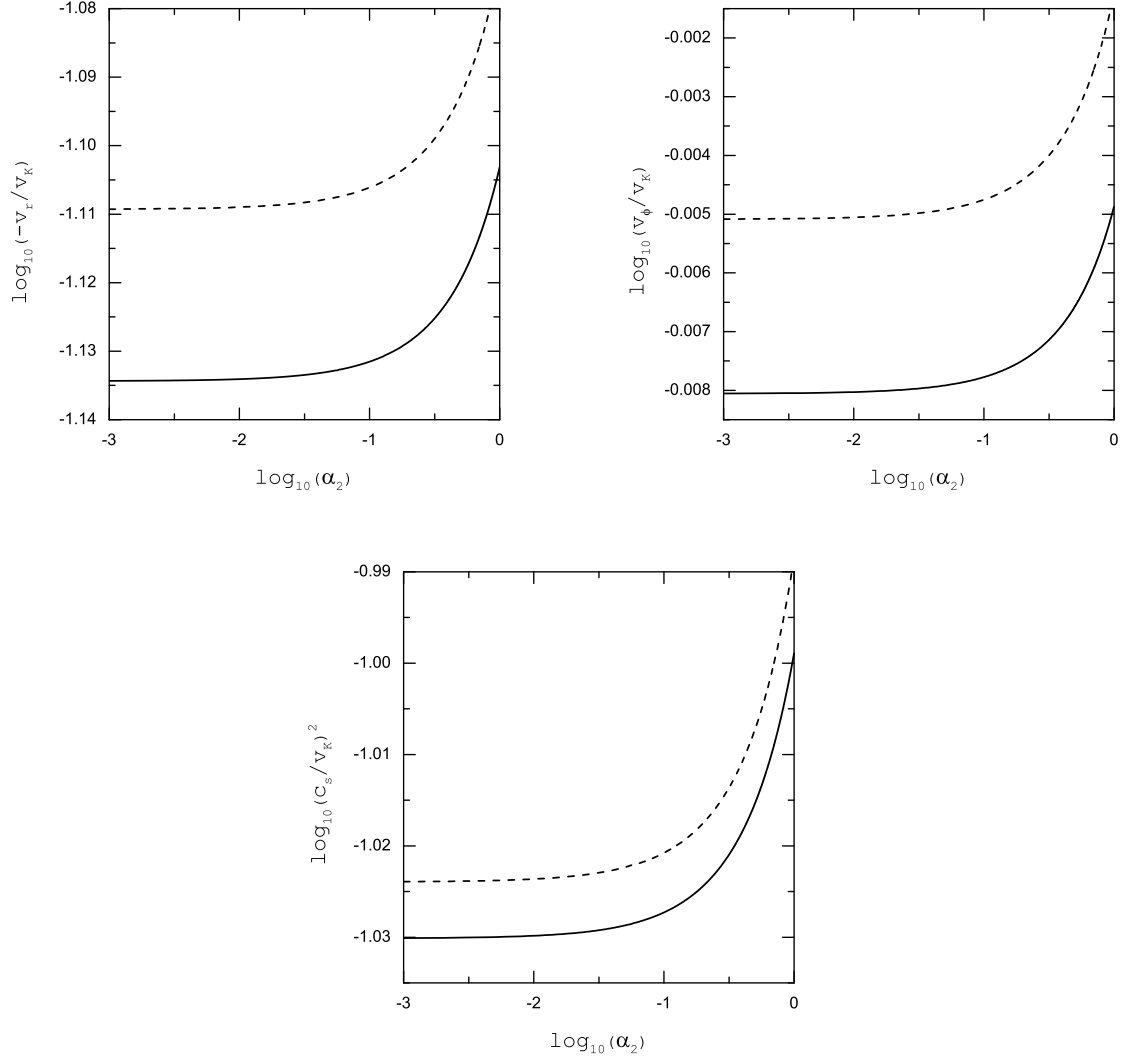


Fig. 3 Similar to Fig. 2. Profiles of the physical variables of the accretion disk versus the strength of anisotropic pressure for different values of β_ϕ when $\eta_0 = 0.1$. The solid and the dashed curves correspond to $\beta_\phi = 0.1$ and 0.2 , respectively

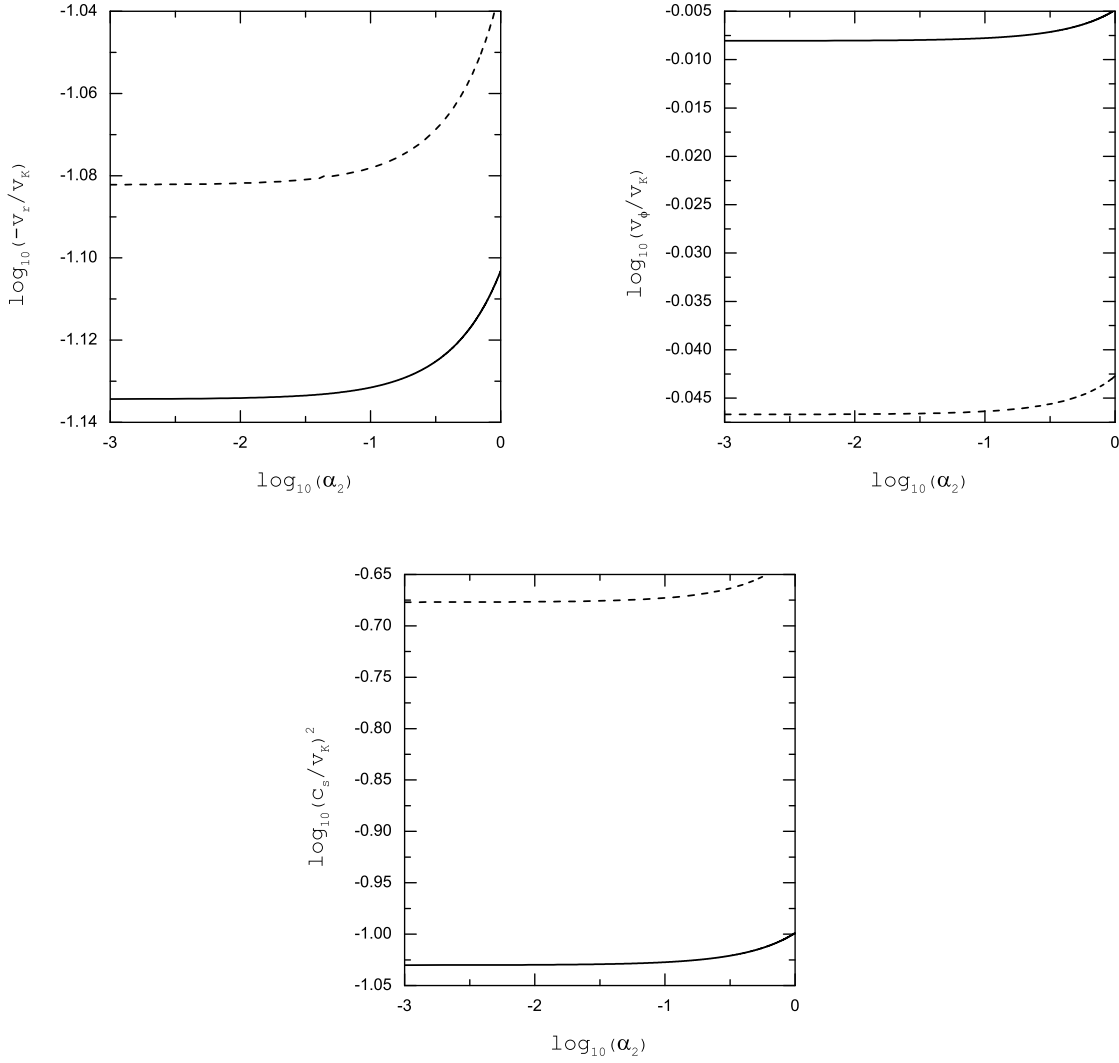


Fig. 4 Similar to Fig. 2. Profiles of the physical variables of the accretion disk versus the strength of anisotropic pressure for different values of s when $\eta_0 = 0.1$. The solid and the dashed curves correspond to $s = 0.5$ and 0.0 , respectively

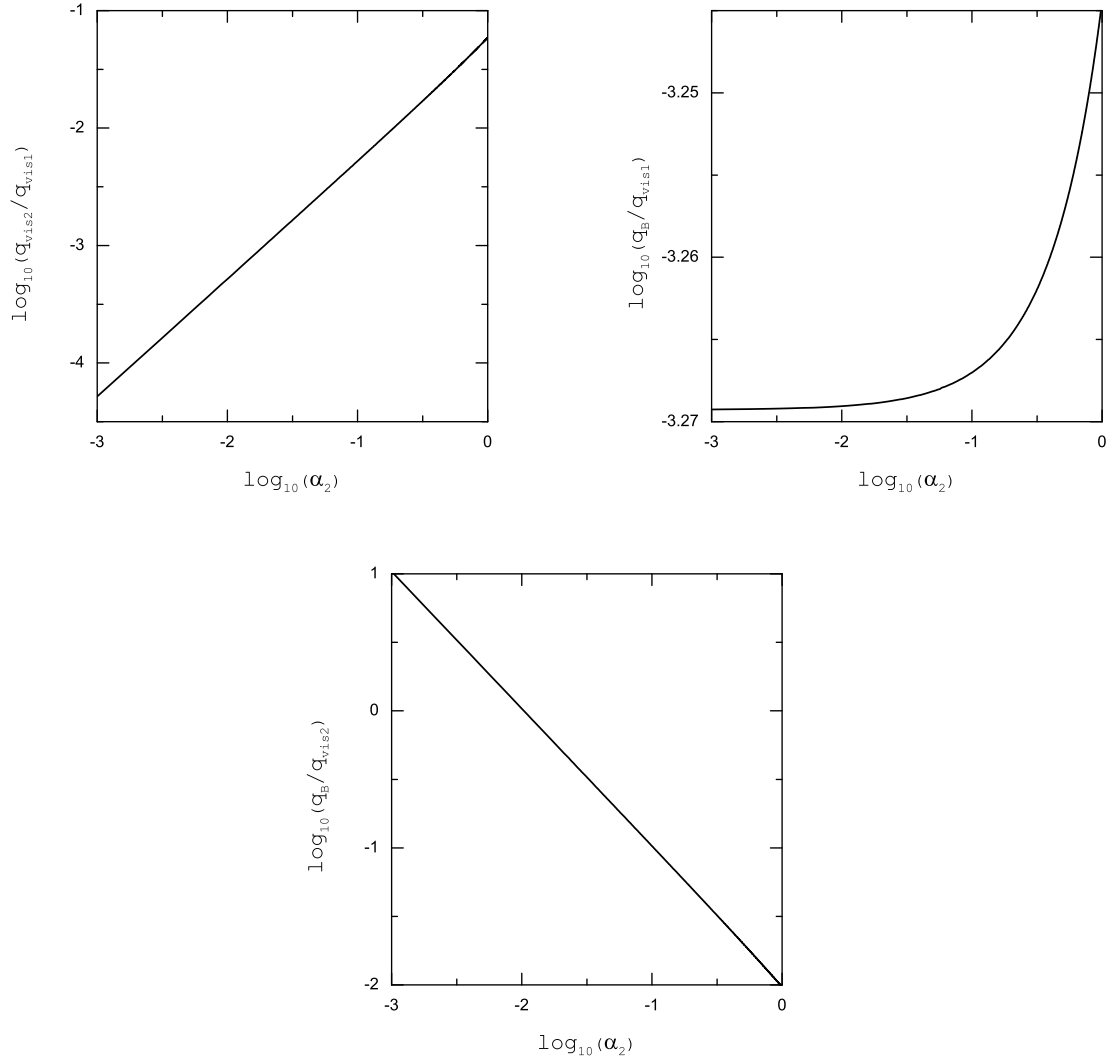


Fig. 5 Profiles of the ratio of heating rates as a function of the strength of anisotropic pressure. We adopt $\eta_0 = 0.1$, $\beta_\phi = 0.1$, and $s = 0.5$

The influence of magnetic diffusivity parameter η_0 is displayed in Fig. 2. Here, the adopted values of the magnetic diffusivity parameter are 0.1 (solid curves) and 1.0 (dashed curves). Noting that the resistive heating is directly related to the η_0 , an increase in the magnetic diffusivity parameter causes the disk to have a higher temperature. Therefore, the sound speed increases with the magnetic diffusivity parameter. According to Eq. (20), the radial velocity also rises. In the absence of anisotropic pressure, Ghoreyshi (2020) also suggested that the radial velocity and the sound speed increase with the magnetic diffusivity. In the present paper, we find that these results depend on the strength of anisotropic pressure. In the low- α_2 limit, the influence of magnetic diffusivity parameter is more significant. We also find that an increase in the magnetic diffusivity parameter causes the disk to rotate with a slower rate (see Eq. (19)).

In Fig. 3, we display the role of the ratio of the magnetic to gas pressures β_ϕ for flows with $\eta_0 = 0.1$. The solid and the dashed curves are the cases with $\beta_\phi = 0.1$ and 0.2, respectively. Other input parameters are similar to Fig. 2. According to Eq. (17), the assumed heating rates depend directly on β_ϕ . The dependence of the heating rates on the ratio of the magnetic to gas pressures causes the disk temperature to increase with β_ϕ , and thus the sound speed to be enhanced. One can see that the anisotropic stress depends on the ratio of the magnetic to gas pressures β_ϕ (see Eq. (15)). Particle-in-cell simulations of the magnetorotational instability (MRI) in collisionless plasmas have also indicated that the importance of the anisotropic stress depends on this ratio (Riquelme et al. 2012). The signs of the magnetic force and of the force of the divergence of the anisotropic pressure in Eq. (15) are negative (i.e., they are directed towards the central black hole). Thus, an increase in β_ϕ causes the infall velocity to rise (see also Eq. (20)). The dependence of the rotational velocity on β_ϕ and C_1 implies that the disks with stronger magnetic field rotate in a faster rate (see Eq. (19)). These results are in excellent agreement with previous work (e.g., Zhang and Dai 2008; Ghoreyshi and Shadmehri 2020; Ghoreyshi 2020).

Now, we explore the effects of s on the physical variables of hot accretion flows when $\eta_0 = 0.1$. In Fig. 4, we set $s = 0.5$ (solid curves) and $s = 0.0$ (dashed curves). The other parameters are similar to Fig. 2. In this paper, we consider the case for which the specific velocities and internal energy of outflow are different from those of inflow ($\zeta_i s \neq 1$). Thus, the internal energy can be taken away from the disk by the outflow. When outflows are stronger, i.e., higher s , the value of

$d\dot{M}/dr$ becomes higher. Hence, higher values of the internal energy are extracted and the disk temperature falls strongly. The reduction of the disk temperature leads to a decrease in the sound speed and in the infall velocity. From Eq. (19), we see that a decrease in the infall velocity enhances the rotational velocity.

As the next step toward a more complete description of resistive disks, we display the ratio of different heating rates as a function of α_2 . The top left panel of Fig. 5 shows the ratio $q_{\text{vis}2}/q_{\text{vis}1}$. We find that the increase in $\log(q_{\text{vis}1}/q_{\text{vis}1})$ with $\log(\alpha_2)$ is linear (with slope 1.03). One can see that the heating due to the anisotropic pressure $q_{\text{vis}2}$ in the low- α_2 limit is negligible compared to $q_{\text{vis}1}$. However, the heating rate $q_{\text{vis}2}$ can be significant in the opposite limit. The ratio $q_B/q_{\text{vis}1}$ is illustrated in the top right panel of Fig. 5. A good fit to the profile shown in this panel over a wide range of α_2 -values is an exponential function. In the top panels of Fig. 5, one can see that the heating rates q_B and $q_{\text{vis}2}$ increase with the strength of the anisotropic pressure. But these two panels show that $q_{\text{vis}1}$ is a dominant heating rate over the two heating rates. On the other hand, our results indicate that the profile of $\log(q_B/q_{\text{vis}2})$ as a function of $\log(\alpha_2)$ is linear. Although the profile of $\log(q_{\text{vis}1}/q_{\text{vis}1})$ has a positive slope, the slope of $\log(q_B/q_{\text{vis}2})$ is negative with a value of about -1.02 . In low- α_2 limit, the resistive heating is more significant than the heating due to the anisotropic pressure (a factor of 10). Thereby, the role of magnetic diffusivity is more important in low- α_2 limit (see also Fig. 2).

5 Summary and discussion

In hot accretion flows, the ions' mean-free path is larger than its Larmor radius. Under these conditions, the pressure parallel to the magnetic field and that perpendicular to the magnetic field are not the same. In such collisionless flows, the pressure anisotropies may be produced by the amplification of the magnetic field by MRI (Sharma et al. 2006; Riquelme et al. 2012). Simulations done by Sharma et al. (2006) have indicated that these anisotropies can be an important agent for angular momentum transport and particle heating (see also Sharma et al. 2007). On the other hand, the magnetic diffusivity also plays a key role in such flows. In this paper, therefore, we studied the dynamics of resistive hot accretion flows with the anisotropic pressure. The toroidal field component was adopted and a modified viscosity form was introduced in Sect. 2. We considered a steady state flow and presented the self-similar solutions described by a function of the radial distance.

We found that the modified viscosity form leads to infall velocities which are quite different from the results of [Bu et al. \(2019\)](#). Our self-similar solutions in the presence of outflows indicated that the magnetic diffusivity causes the infall velocity to increase. Other parameters, such as the strength of the anisotropic pressure and the ratio of the magnetic to gas pressures, can also play a key role in the modification of the infall velocity. In the high- α_2 limit, for example, the radial velocity of inflow rises strongly. Simulations of MRI have also demonstrated that the anisotropic pressure in collisionless plasmas causes the angular momentum transport, and thus the radial velocity, to be enhanced. On the other hand, [Kempski et al. \(2019\)](#) pointed out that the angular momentum transport depends not only on the anisotropic pressure, but also on the magnetic dissipation. Since the disk material in the presence of these mechanisms is able to move inward with faster rate, one can expect that the accretion rate of a hot accretion flow is also modified. The change in accretion rate can alter the black hole luminosity ([Bu and Yang 2019](#)). A significant caveat here is that we did not consider the poloidal magnetic field. Previous work showed that in the ideal MHD the vertical component of the magnetic field reduces the velocities discussed in this paper (e.g., [Mosallanezhad et al. 2013](#)). However, the effect of the vertical field component on the resistive disks structure depends on the magnetic diffusivity ([Ghoreyshi 2020](#)). Then accounting for this component may yield different results.

We found that the rotational velocity and the sound speed are almost unchanged by the modified viscosity form. The rotational velocity changes insensitively with the magnetic diffusivity parameter. Our results showed that the input parameters such as α_2 , β_ϕ , and s can modify the rotational velocity. When outflows are stronger, the sound speed decreases. [Bu et al. \(2019\)](#) also found that stronger outflows lead to a decrease in the sound speed. In the presence of magnetic diffusivity and anisotropic pressure, however, the disk temperature increases. An increase in the disk temperature can lead to heating and acceleration of the electrons. Simulations in collisionless plasmas have also showed that the viscous heating associated with the anisotropic pressure can be an additional mechanism for the heating of electrons ([Sharma et al. 2007](#); [Riquelme et al. 2012](#); [Kempski et al. 2019](#)). The heated and accelerated electrons may be the origin of observed fluctuations (flares) in the infrared and X-ray bands of Sgr A*. [Ding et al. \(2010\)](#) also proposed that the resistive heating may be helpful in heating of the electrons. We also suggest that the magnetic diffusivity and the anisotropic pressure can help to explain non-thermal emission in the form of flares in Sgr A*.

Acknowledgements

The authors would like to thank an unknown referee for a constructive report. The authors thank Dr. Mark Wardle for a helpful comment.

References

- Abbassi, S., Mosallanezhad, A.: *Astrophys. Space Sci.* **341**(2), 375 (2012). 1205.3888. doi:10.1007/s10509-012-1147-x
- Balbus, S.A.: *Astrophys. J.* **616**(2), 857 (2004). astro-ph/0403678. doi:10.1086/424989
- Beckwith, K., Hawley, J.F., Krolik, J.H.: *Astrophys. J.* **678**(2), 1180 (2008). 0709.3833. doi:10.1086/533492
- Béthune, W., Lesur, G., Ferreira, J.: *Astron. Astrophys.* **600**, 75 (2017). 1612.00883. doi:10.1051/0004-6361/201630056
- Bisnovatyi-Kogan, G.S., Lovelace, R.V.E.: *Astrophys. J. Lett.* **486**(1), 43 (1997). astro-ph/9704208. doi:10.1086/310826
- Bisnovatyi-Kogan, G.S., Ruzmaikin, A.A.: *Astrophys. Space Sci.* **42**(2), 401 (1976). doi:10.1007/BF01225967
- Braginskii, S.I.: *Reviews of Plasma Physics* **1**, 205 (1965)
- Braiding, C.R., Wardle, M.: *Mon. Not. R. Astron. Soc.* **422**(1), 261 (2012). 1109.1370. doi:10.1111/j.1365-2966.2012.20601.x
- Bu, D.-F., Yang, X.-H.: *Astrophys. J.* **871**(2), 138 (2019). doi:10.3847/1538-4357/aaf807
- Bu, D.-F., Wu, M.-C., Yuan, Y.-F.: *Mon. Not. R. Astron. Soc.* **459**(1), 746 (2016). 1603.07407. doi:10.1093/mnras/stw723
- Bu, D.-F., Xu, P.-Y., Zhu, B.-C.: *Universe* **5**(4), 89 (2019). doi:10.3390/universe5040089
- Bu, D.-F., Yuan, F., Stone, J.M.: *Mon. Not. R. Astron. Soc.* **413**(4), 2808 (2011). 1011.5331. doi:10.1111/j.1365-2966.2011.18354.x
- Bu, D.-F., Yuan, F., Xie, F.-G.: *Mon. Not. R. Astron. Soc.* **392**(1), 325 (2009). 0810.1341. doi:10.1111/j.1365-2966.2008.14047.x
- Bu, D.-F., Yuan, F., Gan, Z.-M., Yang, X.-H.: *Astrophys. J.* **818**(1), 83 (2016a). 1510.03124. doi:10.3847/0004-637X/818/1/83
- Bu, D.-F., Yuan, F., Gan, Z.-M., Yang, X.-H.: *Astrophys. J.* **823**(2), 90 (2016b). 1603.09442. doi:10.3847/0004-637X/823/2/90
- Cao, X.: *Astrophys. J.* **817**(1), 71 (2016). 1512.00124. doi:10.3847/0004-637X/817/1/71
- Cao, X., Lai, D.: *Mon. Not. R. Astron. Soc.* **485**(2), 1916 (2019). 1712.09265. doi:10.1093/mnras/stz580
- Chandra, M., Gammie, C.F., Foucart, F., Quataert, E.: *Astrophys. J.* **810**(2), 162 (2015). 1508.00878. doi:10.1088/0004-637X/810/2/162
- Cheung, E., Bundy, K., Cappellari, M., Peirani, S., Rujopakarn, W., Westfall, K., Yan, R., Bershady, M., Greene, J.E., Heckman, T.M., Drory, N., Law, D.R., Masters, K.L., Thomas, D., Wake, D.A., Weijmans, A.-M., Rubin, K., Belfiore, F., Vulcani, B., Chen, Y.-M., Zhang, K., Gelfand, J.D., Bizyaev, D., Roman-Lopes, A., Schneider, D.P.: *Nature* **533**(7604), 504 (2016). 1605.07626. doi:10.1038/nature18006
- Crenshaw, D.M., Kraemer, S.B.: *Astrophys. J.* **753**(1), 75 (2012). 1204.6694. doi:10.1088/0004-637X/753/1/75
- Das, I., Basu, S.: *Astrophys. J.* **910**(2), 163 (2021). 2011.08876. doi:10.3847/1538-4357/abdb2c
- De Villiers, J.-P., Hawley, J.F., Krolik, J.H.: *Astrophys. J.* **599**(2), 1238 (2003). astro-ph/0307260. doi:10.1086/379509
- Ding, J., Yuan, F., Liang, E.: *Astrophys. J.* **708**(2), 1545 (2010). 0911.4560. doi:10.1088/0004-637X/708/2/1545
- Done, C., Gierliński, M., Kubota, A.: *Astron. Astrophys. Rev.* **15**(1), 1 (2007). 0708.0148. doi:10.1007/s00159-007-0006-1
- Fendt, C., Čemeljić, M.: *Astron. Astrophys.* **395**, 1045 (2002). astro-ph/0210082. doi:10.1051/0004-6361:20021442
- Fleming, T.P., Stone, J.M., Hawley, J.F.: *Astrophys. J.* **530**(1), 464 (2000). astro-ph/0001164. doi:10.1086/308338
- Ghoreyshi, S.M.: *Proc. Astron. Soc. Aust.* **37**, 023 (2020). 2004.14757. doi:10.1017/pasa.2020.14
- Ghoreyshi, S.M., Shadmehri, M.: *Mon. Not. R. Astron. Soc.* (2020). 2003.04752. doi:10.1093/mnras/staa599
- Gravity Collaboration, Abuter, R., Amorim, A., Bauböck, M., Berger, J.P., Bonnet, H., Brandner, W., Clénet, Y., Coudé Du Foresto, V., de Zeeuw, P.T., Deen, C., Dexter, J., Duvert, G., Eckart, A., Eisenhauer, F., Förster Schreiber, N.M., Garcia, P., Gao, F., Gendron, E., Genzel, R., Gillessen, S., Guajardo, P., Habibi, M., Haubois, X., Henning, T., Hippler, S., Horrobin, M., Huber, A., Jiménez-Rosales, A., Jocou, L., Kervella, P., Lacour, S., Lapeyrère, V., Lazareff, B., Le Bouquin, J.-B., Léna, P., Lippa, M., Ott, T., Panduro, J., Paurmard, T., Perraut, K., Perrin, G., Pfuhl, O., Plewa, P.M., Rabien, S., Rodríguez-Coira, G., Rousset, G., Sternberg, A., Straub, O., Straubmeier, C., Sturm, E., Tacconi, L.J., Vincent, F., von Fellenberg, S., Waisberg, I., Widmann, F., Wiegrecht, E., Wieszorrek, E., Woillez, J., Yazici, S.: *Astron. Astrophys.* **618**, 10 (2018). 1810.12641. doi:10.1051/0004-6361/201834294
- Hirose, S., Krolik, J.H., De Villiers, J.-P., Hawley, J.F.: *Astrophys. J.* **606**(2), 1083 (2004). astro-ph/0311500. doi:10.1086/383184
- Homan, J., Neilsen, J., Allen, J.L., Chakrabarty, D., Fender, R., Fridriksson, J.K., Remillard, R.A., Schulz, N.: *Astrophys. J. Lett.* **830**(1), 5 (2016). 1606.07954. doi:10.3847/2041-8205/830/1/L5
- Igumenshchev, I.V., Narayan, R., Abramowicz, M.A.: *Astrophys. J.* **592**(2), 1042 (2003). astro-ph/0301402. doi:10.1086/375769
- Kato, S., Fukue, J., Mineshige, S.: *Black-Hole Accretion Disks — Towards a New Paradigm —*, (2008)
- Kempki, P., Quataert, E., Squire, J., Kunz, M.W.: *Mon. Not. R. Astron. Soc.* **486**(3), 4013 (2019). 1901.04504. doi:10.1093/mnras/stz1111
- Knigge, C.: *Mon. Not. R. Astron. Soc.* **309**, 409 (1999). astro-ph/9906194. doi:10.1046/j.1365-8711.1999.02839.x
- Kuwabara, T., Shibata, K., Kudoh, T., Matsumoto, R.: *Publ. Astron. Soc. Jpn.* **52**, 1109 (2000). astro-ph/0011165. doi:10.1093/pasj/52.6.1109
- Ma, R.-Y., Roberts, S.R., Li, Y.-P., Wang, Q.D.: *Mon. Not. R. Astron. Soc.* **483**(4), 5614 (2019). 1811.02190. doi:10.1093/mnras/sty3039
- Mori, S., Bai, X.-N., Okuzumi, S.: *Astrophys. J.* **872**(1), 98 (2019). 1901.06921. doi:10.3847/1538-4357/ab0022
- Mosallanezhad, A., Khajavi, M., Abbassi, S.: *Research in Astronomy and Astrophysics* **13**(1), 87 (2013). 1206.2841. doi:10.1088/1674-4527/13/1/009

- Narayan, R., Yi, I.: *Astrophys. J. Lett.* **428**, 13 (1994). [astro-ph/9403052](https://doi.org/10.1086/187381). doi:10.1086/187381
- Ohsuga, K., Mineshige, S., Mori, M., Kato, Y.: *Publ. Astron. Soc. Jpn.* **61**(3), 7 (2009). 0903.5364. doi:10.1093/pasj/61.3.47
- Pandey, B.P., Wardle, M.: *Mon. Not. R. Astron. Soc.* **385**(4), 2269 (2008). 0707.2688. doi:10.1111/j.1365-2966.2008.12908.x
- Park, J., Hada, K., Kino, M., Nakamura, M., Ro, H., Trippe, S.: *Astrophys. J.* **871**(2), 257 (2019). 1812.08386. doi:10.3847/1538-4357/aaf9a9
- Parrish, I.J., Stone, J.M.: *Astrophys. J.* **664**(1), 135 (2007). [astro-ph/0612195](https://doi.org/10.1086/518881). doi:10.1086/518881
- Pudritz, R.E.: *Astrophys. J.* **293**, 216 (1985). doi:10.1086/163227
- Qian, Q., Fendt, C., Vourellis, C.: *Astrophys. J.* **859**(1), 28 (2018). 1804.09652. doi:10.3847/1538-4357/aabd36
- Qiao, E., Liu, B.F.: *Publ. Astron. Soc. Jpn.* **61**, 403 (2009). 0901.0475. doi:10.1093/pasj/61.2.403
- Quataert, E.: *Astrophys. J.* **500**(2), 978 (1998). [astro-ph/9710127](https://doi.org/10.1086/305770). doi:10.1086/305770
- Quataert, E., Dorland, W., Hammett, G.W.: *Astrophys. J.* **577**(1), 524 (2002). [astro-ph/0205492](https://doi.org/10.1086/342174). doi:10.1086/342174
- Ripperda, B., Bacchini, F., Porth, O., Most, E.R., Olivares, H., Nathanael, A., Rezzolla, L., Teunissen, J., Keppens, R.: *Astrophys. J. Suppl. Ser.* **244**(1), 10 (2019a). 1907.07197. doi:10.3847/1538-4365/ab3922
- Ripperda, B., Porth, O., Sironi, L., Keppens, R.: *Mon. Not. R. Astron. Soc.* **485**(1), 299 (2019b). 1810.10116. doi:10.1093/mnras/stz387
- Ripperda, B., Bacchini, F., Philippov, A.A.: *Astrophys. J.* **900**(2), 100 (2020). 2003.04330. doi:10.3847/1538-4357/ababab
- Riquelme, M.A., Quataert, E., Sharma, P., Spitkovsky, A.: *Astrophys. J.* **755**(1), 50 (2012). 1201.6407. doi:10.1088/0004-637X/755/1/50
- Samadi, M., Abbassi, S., Khajavi, M.: *Mon. Not. R. Astron. Soc.* **437**(4), 3124 (2014). 1310.6317. doi:10.1093/mnras/stt2052
- Sano, T., Stone, J.M.: *Astrophys. J.* **570**(1), 314 (2002). [astro-ph/0201179](https://doi.org/10.1086/339504). doi:10.1086/339504
- Scepi, N., Lesur, G., Dubus, G., Flock, M.: *Astron. Astrophys.* **609**, 77 (2018). 1710.05872. doi:10.1051/0004-6361/201731900
- Shadmehri, M.: *Astron. Astrophys.* **424**, 379 (2004). [astro-ph/0303220](https://doi.org/10.1051/0004-6361:20040538). doi:10.1051/0004-6361:20040538
- Shakura, N.I., Sunyaev, R.A.: *Astron. Astrophys.* **24**, 337 (1973)
- Sharma, P., Quataert, E., Stone, J.M.: *Mon. Not. R. Astron. Soc.* **389**(4), 1815 (2008). 0804.1353. doi:10.1111/j.1365-2966.2008.13686.x
- Sharma, P., Hammett, G.W., Quataert, E.: *Astrophys. J.* **596**(2), 1121 (2003). [astro-ph/0305486](https://doi.org/10.1086/378234). doi:10.1086/378234
- Sharma, P., Hammett, G.W., Quataert, E., Stone, J.M.: *Astrophys. J.* **637**(2), 952 (2006). [astro-ph/0508502](https://doi.org/10.1086/498405). doi:10.1086/498405
- Sharma, P., Quataert, E., Hammett, G.W., Stone, J.M.: *Astrophys. J.* **667**(2), 714 (2007). [astro-ph/0703572](https://doi.org/10.1086/520800). doi:10.1086/520800
- Tombesi, F., Sambruna, R.M., Reeves, J.N., Braitto, V., Ballo, L., Gofford, J., Cappi, M., Mushotzky, R.F.: *Astrophys. J.* **719**(1), 700 (2010). 1006.3536. doi:10.1088/0004-637X/719/1/700
- Tombesi, F., Tazaki, F., Mushotzky, R.F., Ueda, Y., Cappi, M., Gofford, J., Reeves, J.N., Guainazzi, M.: *Mon. Not. R. Astron. Soc.* **443**(3), 2154 (2014). 1406.7252. doi:10.1093/mnras/stu1297
- Čemeljčić, M., Vlahakis, N., Tsinganos, K.: *Mon. Not. R. Astron. Soc.* **442**(2), 1133 (2014). 1405.3924. doi:10.1093/mnras/stu952
- Vourellis, C., Fendt, C., Qian, Q., Noble, S.C.: *Astrophys. J.* **882**(1), 2 (2019). 1907.10622. doi:10.3847/1538-4357/ab32e2
- Wang, L., Bai, X.-N., Goodman, J.: *Astrophys. J.* **874**(1), 90 (2019). 1810.12330. doi:10.3847/1538-4357/ab06fd
- Wang, Q.D., Nowak, M.A., Markoff, S.B., Baganoff, F.K., Nayakshin, S., Yuan, F., Cuadra, J., Davis, J., Dexter, J., Fabian, A.C., Grosso, N., Haggard, D., Houck, J., Ji, L., Li, Z., Neilsen, J., Porquet, D., Ripple, F., Shcherbakov, R.V.: *Science* **341**(6149), 981 (2013). 1307.5845. doi:10.1126/science.1240755
- Wu, M.-C., Bu, D.-F., Gan, Z.-M., Yuan, Y.-F.: *Astron. Astrophys.* **608**, 114 (2017). doi:10.1051/0004-6361/201730803
- Xue, L., Wang, J.: *Astrophys. J.* **623**, 372 (2005). doi:10.1086/428338
- Yan, Z., Yu, W.: *Mon. Not. R. Astron. Soc.* **470**(4), 4298 (2017). 1706.06472. doi:10.1093/mnras/stx1562
- Yuan, F., Narayan, R.: *Annu. Rev. Astron. Astrophys.* **52**, 529 (2014). 1401.0586. doi:10.1146/annurev-astro-082812-141003
- Yuan, F., Bu, D., Wu, M.: *Astrophys. J.* **761**, 130 (2012). 1206.4173. doi:10.1088/0004-637X/761/2/130
- Yuan, F., Markoff, S., Falcke, H.: *Astron. Astrophys.* **383**, 854 (2002). [astro-ph/0112464](https://doi.org/10.1051/0004-6361:20011709). doi:10.1051/0004-6361:20011709
- Yuan, F., Wu, M., Bu, D.: *Astrophys. J.* **761**, 129 (2012). 1206.4157. doi:10.1088/0004-637X/761/2/129
- Yuan, F., Gan, Z., Narayan, R., Sadowski, A., Bu, D., Bai, X.-N.: *Astrophys. J.* **804**, 101 (2015). 1501.01197. doi:10.1088/0004-637X/804/2/101
- Yuan, F., Yoon, D., Li, Y.-P., Gan, Z.-M., Ho, L.C., Guo, F.: *Astrophys. J.* **857**(2), 121 (2018). 1712.04964. doi:10.3847/1538-4357/aab8f8
- Zahra Zeraatgari, F., Mosallanezhad, A., Abbassi, S., Yuan, Y.-F.: *Astrophys. J.* **852**(2), 124 (2018). 1712.03078. doi:10.3847/1538-4357/aa9fffd
- Zanni, C., Ferrari, A., Rosner, R., Bodo, G., Massaglia, S.: *Astron. Astrophys.* **469**(3), 811 (2007). [astro-ph/0703064](https://doi.org/10.1051/0004-6361:20066400). doi:10.1051/0004-6361:20066400
- Zhang, D., Dai, Z.G.: *Mon. Not. R. Astron. Soc.* **388**(3), 1409 (2008). 0805.3254. doi:10.1111/j.1365-2966.2008.13483.x
- Zhang, S.-N., Liao, J., Yao, Y.: *Mon. Not. R. Astron. Soc.* **421**(4), 3550 (2012). 1201.3451. doi:10.1111/j.1365-2966.2012.20579.x